

## Implications of $A_4$ modular symmetry on neutrino mass, mixing and leptogenesis with Linear seesaw

---

Rukmani Mohanta,<sup>a,\*</sup> Mitesh K Behera,<sup>a</sup> S. Singirala<sup>a</sup> and S. Mishra<sup>b</sup>

<sup>a</sup>*School of Physics, University of Hyderabad, Hyderabad - 500046, India*

<sup>b</sup>*Physics Department, IIT Hyderabad, Kandi - 502285, India*

*E-mail: [rmsp@uohyd.ac.in](mailto:rmsp@uohyd.ac.in), [miteshbehera1304@gmail.com](mailto:miteshbehera1304@gmail.com),  
[krishnas542@gmail.com](mailto:krishnas542@gmail.com), [subhasmita.mishra92@gmail.com](mailto:subhasmita.mishra92@gmail.com)*

Motivated by the crucial role played by the discrete flavour symmetry groups in explaining the observed neutrino oscillation data, we consider the application  $A_4$  modular symmetry in the linear seesaw framework. The basic idea behind using the modular symmetry is to minimize the usage of multiple flavon fields having specific vacuum expectation value (VEV) alignments. The breaking of flavor symmetry takes place when the complex modulus  $\tau$  acquires VEV. Linear seesaw in this framework is realized with six heavy  $SU(2)_L$  singlet fermion superfields and a weighton. We discuss the phenomena of neutrino mixing and show that the obtained mixing angles and CP violating phase in this framework are compatible with the observed  $3\sigma$  range of the current oscillation data. In addition, we also investigate the phenomenon of leptogenesis arising from the decay of lightest heavy fermion superfield to explain the observed baryon asymmetry of the Universe.

*21st Conference on Flavor Physics and CP Violation (FPCP 2023)*

*29 May - 2 June 2023*

*Lyon, France*

---

\*Speaker

## 1. Introduction

The origin of neutrino masses and mixing still remains as one of the open issues. The most popular scenario to generate the light neutrino masses is the canonical or Type-I seesaw, where right-handed neutrinos ( $N_{Ri}$ ), transforming as singlets under standard model gauge group are introduced. In order to explain the eV-scale light neutrinos, the masses of the right-handed neutrinos are supposed to be  $\mathcal{O}(10^{15})$  GeV, which are obviously beyond the reach of current and future experiments. However, the seesaw scale can be lowered to TeV range, if one includes three additional left-handed sterile neutrinos ( $S_{Li}$ ), in conjunction with the three right-handed neutrinos. This mechanism is known as linear or inverse seesaw depending on the structure of the neutrino mass matrix in the  $(\nu_L, N_R, S_L^c)$  basis.

In general, to implement the low-scale seesaw mechanisms, certain symmetries are assumed, like discrete flavour symmetries  $A_4$ ,  $S_3$ ,  $S_4$ , etc., to avoid certain unwanted terms in the extended neutrino mass matrix of  $(\nu_L^c, N_{Ri}, S_{Li}^c)^T$  basis. However, a number of flavon fields are required for the breaking of these flavor symmetries as well as to accommodate the observed neutrino oscillation data. Additionally, the vacuum alignment of these flavon fields pose a challenging task. However, these issues can be avoided by introducing the modular symmetry in addition to the discrete flavor symmetry as discussed in Refs. [1, 2]. In recent times, modular symmetry [3–5] has gained the pace and is in the limelight. The advantage of modular symmetry is that it restricts the usage of excess flavon fields, where, the role of flavons is performed by Yukawa couplings, which are holomorphic function of modulus  $\tau$ . When this modulus acquires the vacuum expectation value (VEV), it breaks the flavor symmetry. In this work, we would like to study the neutrino phenomenology and leptogenesis in the context of discrete  $A_4$  modular symmetry [6]. Modular symmetries have been impeccable in neutrino and quark sectors as the Yukawa couplings transform non-trivially under  $A_4$  symmetry, that helps to explore the neutrino phenomenology with a specific flavor structure of the mass matrix.

The outline of the paper is as follows. In Sec.2, we outline the model framework that provides the well known linear seesaw mechanism with discrete  $A_4$ -modular symmetry. In Sec.3, numerical correlational study between different observables of neutrino sector is established. Leptogenesis in the context of the present model is discussed in Sec.4. Finally in Sec. 5, we conclude our results.

## 2. Model Framework

Here, we introduce the model framework for investigating the impact of  $A_4$  modular symmetry on neutrino phenomenology and leptogenesis. The standard model is extended with discrete  $A_4$  modular symmetry and a global  $U(1)_X$  symmetry is imposed to forbid certain unwanted terms in the superpotential. The particle spectrum is enriched with six extra singlet heavy fermion superfields ( $N_{Ri}$  and  $S_{Li}$ ) and one weighton field ( $\rho$ ). The extra supermultiplets of the model transform as triplet under the  $A_4$  modular group. The  $A_4$  and  $U(1)_X$  symmetries are considered to be broken at a scale much higher than the electroweak symmetry breaking. The charges under  $SU(2)_L \times U(1)_Y \times U(1)_X \times A_4$  are shown below in Table 1, where  $k_I$  being the modular weight. Additionally, the Yukawa coupling  $\mathbf{Y} = (y_1, y_2, y_3)$  transforms as a triplet under  $A_4$  symmetry with modular weight 2. The modular forms of the Yukawa coupling  $\mathbf{Y}$  can be expressed in terms of

Dedekind eta-function  $\eta(\tau)$  and its derivative [3] as

$$\begin{aligned}
 y_1(\tau) &= \frac{i}{2\pi} \left( \frac{\eta'(\tau/3)}{\eta(\tau/3)} + \frac{\eta'((\tau+1)/3)}{\eta((\tau+1)/3)} + \frac{\eta'((\tau+2)/3)}{\eta((\tau+2)/3)} - \frac{27\eta'(3\tau)}{\eta(3\tau)} \right), \\
 y_2(\tau) &= \frac{-i}{\pi} \left( \frac{\eta'(\tau/3)}{\eta(\tau/3)} + \omega^2 \frac{\eta'((\tau+1)/3)}{\eta((\tau+1)/3)} + \omega \frac{\eta'((\tau+2)/3)}{\eta((\tau+2)/3)} \right), \\
 y_3(\tau) &= \frac{-i}{\pi} \left( \frac{\eta'(\tau/3)}{\eta(\tau/3)} + \omega \frac{\eta'((\tau+1)/3)}{\eta((\tau+1)/3)} + \omega^2 \frac{\eta'((\tau+2)/3)}{\eta((\tau+2)/3)} \right).
 \end{aligned} \tag{1}$$

Fields	$e_R^c$	$\mu_R^c$	$\tau_R^c$	$L_L$	$N_R$	$S_L^c$	$H_{u,d}$	$\rho$
$SU(2)_L$	1	1	1	2	1	1	2	1
$U(1)_Y$	1	1	1	-1/2	0	0	1/2, -1/2	0
$U(1)_X$	1	1	1	-1	1	-2	0	1
$A_4$	1	1'	1''	1, 1'', 1'	3	3	1	1
$k_I$	1	1	1	-1	-1	-1	0	0

**Table 1:** Particle content of the model and their charges under  $SU(2)_L \times U(1)_Y \times U(1)_X \times A_4$  where  $k_I$  is the modular weight.

To obtain the light active neutrino masses in the linear seesaw framework, we need to determine the extended mass matrix in the flavor basis of  $(\nu_L, N_R, S_L^c)$  is expressed as

$$\mathbb{M} = \begin{pmatrix} 0 & M_D & M_{LS} \\ M_D^T & 0 & M_{RS} \\ M_{LS}^T & M_{RS}^T & 0 \end{pmatrix}. \tag{2}$$

The resulting light neutrino mass formula can be obtained in the limit  $M_{RS} \gg M_D, M_{LS}$  as,

$$m_\nu = M_D M_{RS}^{-1} M_{LS}^T + \text{transpose}. \tag{3}$$

The Dirac mass matrix of the light neutrinos  $M_D$  can be obtained from the superpotential

$$\mathcal{W}_D = \alpha_D \bar{L}_{eL} H_u (Y N_R)_1 + \beta_D \bar{L}_{\mu L} H_u (Y N_R)_{1'} + \gamma_D \bar{L}_{\tau L} H_u (Y N_R)_{1''}, \tag{4}$$

and can be expressed as

$$M_D = \frac{\nu_u}{\sqrt{2}} \begin{bmatrix} \alpha_D & 0 & 0 \\ 0 & \beta_D & 0 \\ 0 & 0 & \gamma_D \end{bmatrix} \begin{bmatrix} y_1 & y_3 & y_2 \\ y_2 & y_1 & y_3 \\ y_3 & y_2 & y_1 \end{bmatrix}_{LR}. \tag{5}$$

Analogously, the pseudo-Dirac mass matrix can be obtained from the superpotential having the form

$$\mathcal{W}_{LS} = \left[ \alpha'_D L_{eL} H_u (Y S_L^c)_1 + \beta'_D L_{\mu L} H_u (Y S_L^c)_{1'} + \gamma'_D L_{\tau L} H_u (Y S_L^c)_{1''} \right] \frac{\rho^3}{\Lambda^3}, \tag{6}$$

$$M_{LS} = \frac{v_u}{\sqrt{2}} \left( \frac{v_\rho}{\sqrt{2}\Lambda} \right)^3 \begin{bmatrix} \alpha'_D & 0 & 0 \\ 0 & \beta'_D & 0 \\ 0 & 0 & \gamma'_D \end{bmatrix} \begin{bmatrix} y_1 & y_3 & y_2 \\ y_2 & y_1 & y_3 \\ y_3 & y_2 & y_1 \end{bmatrix}_{LR}. \quad (7)$$

The mixing between the two heavy fermions originates from the interaction term

$$\mathcal{W}_{M_{RS}} = [\alpha_{SN} \mathbf{Y}(\overline{S_L} N_R)_{\text{symm}} + \beta_{SN} \mathbf{Y}(\overline{S_L} N_R)_{\text{Anti-symm}}] \rho, \quad (8)$$

and using  $\langle \rho \rangle = v_\rho / \sqrt{2}$ , the corresponding mass matrix can be expressed as

$$M_{RS} = \frac{v_\rho}{\sqrt{2}} \left( \frac{\alpha_{NS}}{3} \begin{bmatrix} 2y_1 & -y_3 & -y_2 \\ -y_3 & 2y_2 & -y_1 \\ -y_2 & -y_1 & 2y_3 \end{bmatrix} + \beta_{NS} \begin{bmatrix} 0 & y_3 & -y_2 \\ -y_3 & 0 & y_1 \\ y_2 & -y_1 & 0 \end{bmatrix} \right). \quad (9)$$

The masses for the heavy fermions can be found in the basis  $(N_R, S_L^c)^T$  as,

$$M_{Hf} = \begin{pmatrix} 0 & M_{RS} \\ M_{RS}^T & 0 \end{pmatrix}, \quad (10)$$

which leads to six doubly degenerate mass eigenstates for the heavy fermions upon diagonalization.

### 3. Numerical Analysis

For numerical analysis, we use the values of the oscillation parameters from the global fit data [7]. Here, we numerically diagonalize the neutrino mass matrix (3) through the relation  $U^\dagger \mathcal{M} U = \text{diag}(m_1^2, m_2^2, m_3^2)$ , where  $\mathcal{M} = m_\nu m_\nu^\dagger$  and  $U$  is an unitary matrix, from which the neutrino mixing angles can be extracted using the standard relations:

$$\sin^2 \theta_{13} = |U_{13}|^2, \quad \sin^2 \theta_{12} = \frac{|U_{12}|^2}{1 - |U_{13}|^2}, \quad \sin^2 \theta_{23} = \frac{|U_{23}|^2}{1 - |U_{13}|^2}. \quad (11)$$

To accommodate the current oscillation data, we scan the values of the model parameters in the following ranges:

$$\text{Re}[\tau] \in [-0.5, 0.5], \quad \text{Im}[\tau] \in [1, 2], \quad \{\alpha_D, \beta_D, \gamma_D\} \in 10^{-5} [0.1, 1], \quad \{\alpha'_D, \beta'_D, \gamma'_D\} \in 10^{-2} [0.1, 1], \\ \alpha_{NS} \in [0, 0.5], \quad \beta_{NS} \in [0, 0.0001], \quad v_\rho \in [10, 100] \text{ TeV}, \quad \Lambda \in [100, 1000] \text{ TeV}.$$

The input parameters are randomly scanned over the above mentioned ranges and the allowed regions for those are initially constrained by the observed  $3\sigma$  limit of solar and atmospheric mass squared differences and mixing angles and then further constrained by the observed sum of active neutrino masses  $\sum m_i < 0.12$  eV [8]. For normal ordering, the typical range of modulus  $\tau$  is found to be

$$-0.5 \lesssim \text{Re}[\tau] \lesssim 0.5 \quad \text{and} \quad 1 \lesssim \text{Im}[\tau] \lesssim 2. \quad (12)$$

Thus, the values of the Yukawa couplings, which are dependent on  $\tau$ , found to vary in the following ranges,

$$0.99 \lesssim y_1(\tau) \lesssim 1, \quad 0.1 \lesssim y_2(\tau) \lesssim 0.8 \quad \text{and} \quad 0.01 \lesssim y_3(\tau) \lesssim 0.3. \quad (13)$$

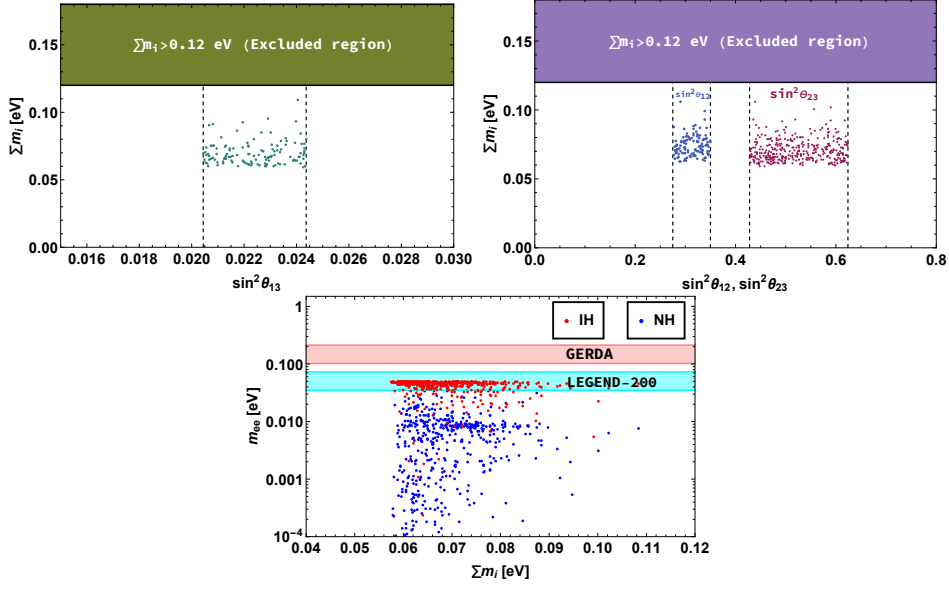


**Figure 1:** Top left (right) panel represents the correlation between  $\sin^2 \theta_{13}$  ( $\sin^2 \theta_{12}$  and  $\sin^2 \theta_{23}$ ) with the sum of active neutrino masses while the bottom panel depicts correlation of effective neutrino mass  $m_{ee}$  with the sum of active neutrino masses.

Variation of the mixing angles with the sum of active neutrino masses, consistent with the allowed  $3\sigma$  range are obtained, as shown in the top left and right panels of Fig. 1. The effective neutrinoless double beta decay mass parameter  $m_{ee} = |m_1 \cos^2 \theta_{12} \cos^2 \theta_{13} + m_2 \sin^2 \theta_{12} \cos^2 \theta_{13} e^{i\alpha_{21}} + m_3 \sin^2 \theta_{13} e^{i(\alpha_{31} - 2\delta_{CP})}|$ , where  $\alpha_{21}$  and  $\alpha_{31}$  are Majorana phases, for both normal and inverted hierarchies is found to have a maximum value of 55 meV from the variation of observed sum of active neutrino masses, which is presented in the bottom panel of Fig. 1. The horizontal pink and cyan bands represent the  $3\sigma$  sensitivity limits of current GERDA and the future LEGEND-200 experiments respectively.

#### 4. Leptogenesis

Understanding the origin of neutrino mass and baryon asymmetry of the Universe (BAU) are two major challenges in Particle Physics. Leptogenesis plays a vital role in relating these two issues. The baryon asymmetry is parameterized in terms of baryon to photon ratio [8],

$$\eta = \frac{n_B - n_{\bar{B}}}{n_\gamma} = (6.12 \pm 0.04) \times 10^{-10}, \quad (14)$$

where  $n_B$ ,  $n_{\bar{B}}$  and  $n_\gamma$  represent the number densities of baryons, antibaryons and photons. Leptogenesis is known to be one of the most preferred scenarios to generate the observed baryon asymmetry of the Universe where the lepton asymmetry is generated through the decay of heavy fermions. For quasi-degenerate heavy Majorana neutrinos, resonant leptogenesis occurs, resulting in a large CP asymmetry. The present model includes six heavy states with doubly degenerate masses for each pair as seen from Eqn.(10). But one can introduce a higher dimensional mass term for the heavy

neutrino ( $S_L^c$ ) as

$$L_M = -\alpha_R Y S_L^c S_L^c \frac{\rho^4}{\Lambda^3}. \quad (15)$$

This leads to a small mass splitting between the heavy fermions, there by enhancing the CP asymmetry to generate required lepton asymmetry [9, 10]. This leads to a small mass splitting between the heavy fermions, there by enhancing the CP asymmetry through the self energy contribution ( $\epsilon$  type CP asymmetry). Thus, one can construct the right-handed Majorana mass matrix as follows

$$M_R = \frac{\alpha_R v_\rho^4}{6\Lambda^3} \begin{pmatrix} 2y_1 & -y_3 & -y_2 \\ -y_3 & 2y_2 & -y_1 \\ -y_2 & -y_1 & 2y_3 \end{pmatrix}. \quad (16)$$

The coupling  $\alpha_R$  is chosen to be extremely small to retain the linear seesaw structure of the mass matrix (2), i.e.,  $M_D, M_{LS} \gg M_R$  and such inclusion does not affect the previous results. However, this term introduces a small mass splitting and the  $2 \times 2$  submatrix of Eqn. (2) in the  $(N_R, S_L^c)$  basis, now can be written as

$$M = \begin{pmatrix} 0 & M_{RS} \\ M_{RS}^T & M_R \end{pmatrix}. \quad (17)$$

Block diagonalization of the above mass matrix (17) yields

$$M' = \begin{pmatrix} M_{RS} + \frac{M_R}{2} & -\frac{M_R}{2} \\ -\frac{M_R}{2} & -M_{RS} + \frac{M_R}{2} \end{pmatrix} \approx \begin{pmatrix} M_{RS} + \frac{M_R}{2} & 0 \\ 0 & -M_{RS} + \frac{M_R}{2} \end{pmatrix}. \quad (18)$$

Therefore, the mass eigenstates ( $N^\pm$ ) are related to  $N_R$  and  $S_L^c$  through

$$\begin{pmatrix} S_{Li}^c \\ N_{Ri} \end{pmatrix} = \begin{pmatrix} \cos \theta & -\sin \theta \\ \sin \theta & \cos \theta \end{pmatrix} \begin{pmatrix} N_i^+ \\ N_i^- \end{pmatrix}. \quad (19)$$

The mass eigenvalues for the new states  $N^+$  and  $N^-$  can be obtained by diagonalizing the block diagonal form of heavy superfield masses, expressed as

$$M_{RS} \pm \frac{M_R}{2} = \left( \frac{\alpha_{NS} v_\rho}{\sqrt{2}} \pm \frac{\alpha_R v_\rho^4}{4\Lambda^3} \right) \begin{pmatrix} 2y_1 & -y_3 & -y_2 \\ -y_3 & 2y_2 & -y_1 \\ -y_2 & -y_1 & 2y_3 \end{pmatrix}. \quad (20)$$

Thus, we get three sets of nearly degenerate mass states after diagonalization. We further assume that the lightest pair with TeV scale masses dominantly contribute to the CP asymmetry.

The evolution of lepton asymmetry can be deduced from the dynamics of relevant Boltzmann equations. Sakharov criteria [11] demand the decay of parent fermion to be out of equilibrium to generate the lepton asymmetry. To impose this condition, one has to compare the Hubble rate with the decay rate as follows

$$K = \frac{\Gamma_{N_1^-}}{H(T = M_1^-)}. \quad (21)$$

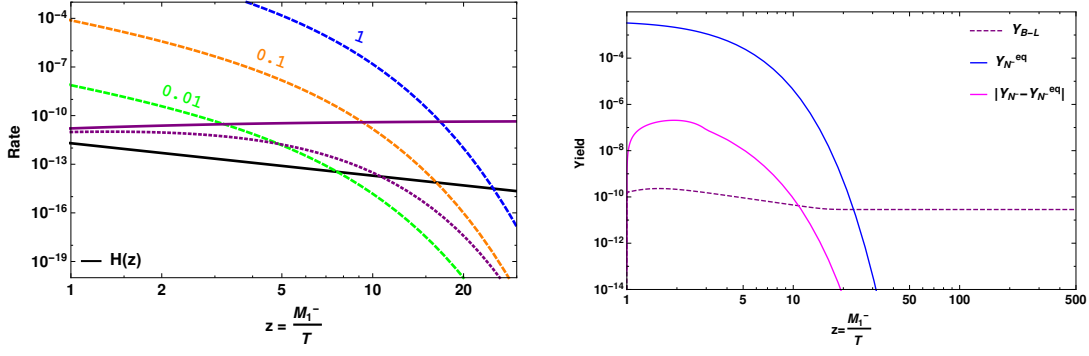


**Figure 2:** Left panel projects the comparison of interaction rates with Hubble expansion, where purple lines correspond to decay (solid), inverse decay (dotted) and scattering rates plotted for various values of Majorana coupling (green, orange, blue). Right panel projects the evolution of  $Y_{B-L}$  (dashed) as a function of  $z = M_1^-/T$ .

Here,  $H = \frac{1.67\sqrt{g_\star} T^2}{M_{\text{Pl}}}$ , with  $M_{\text{Pl}} = 1.22 \times 10^{19}$  GeV and we consider the value of the relativistic degrees of freedom at temperature  $T \sim 1$  TeV, which is roughly same as its SM value i.e.,  $g_\star = 106.75$ , as no new particles have been observed so far up to the TeV scale. The Boltzmann equations for the evolution of the number densities of right-handed fermion and lepton, written in terms of yield parameter (ratio of number density to entropy density) are given by [12–14]

$$\begin{aligned} \frac{dY_{N^-}}{dz} &= -\frac{z}{sH(M_1^-)} \left[ \left( \frac{Y_{N^-}}{Y_{N^-}^{\text{eq}}} - 1 \right) \gamma_D + \left( \left( \frac{Y_{N^-}}{Y_{N^-}^{\text{eq}}} \right)^2 - 1 \right) \gamma_S \right], \\ \frac{dY_{B-L}}{dz} &= -\frac{z}{sH(M_1^-)} \left[ \epsilon_{N^-} \left( \frac{Y_{N^-}}{Y_{N^-}^{\text{eq}}} - 1 \right) \gamma_D - \frac{Y_{B-L}}{Y_\ell^{\text{eq}}} \frac{\gamma_D}{2} \right], \end{aligned} \quad (22)$$

where  $s$  denotes the entropy density,  $z = M_1^-/T$ ,  $Y_{N^-}^{\text{eq}}$  and  $Y_\ell^{\text{eq}}$  are the equilibrium number densities, given in [15].

The interaction rates are compared with Hubble expansion in the left panel of Fig. 2. The decay ( $\Gamma_D$ ) and inverse decay ( $\Gamma_D \frac{Y_{N^-}^{\text{eq}}}{Y_\ell^{\text{eq}}}$ ) rates are plotted in purple with the coupling strength  $\sim 10^{-6}$ . The scattering rate ( $\frac{\gamma_S}{sY_{N^-}^{\text{eq}}}$ ) for  $N_1^- N_1^- \rightarrow \rho\rho$  is projected for various set of values for coupling (of Eq. 8), consistent with neutrino oscillation study. In one-flavor approximation, the solution of Boltzmann eqns (22) using the benchmark value  $\epsilon_{N^-} = -5.5 \times 10^{-4}$ , is projected in the right panel of Fig. 2 with the inclusion of decay and scattering rates. Once the out-of-equilibrium criteria is satisfied, the decay proceeds slow (over abundance),  $Y_{N^-}$  does not trace  $Y_{N^-}^{\text{eq}}$  (magenta curve) and the lepton asymmetry (dashed curve) is generated. The obtained lepton asymmetry gets converted to the observed baryon asymmetry through sphaleron transition, given by [16]

$$Y_B = \left( \frac{8N_f + 4N_H}{22N_f + 13N_H} \right) Y_{B-L}. \quad (23)$$

Using the asymptotic value of  $Y_{B-L}$  as  $8.5 \times 10^{-10}$  from Fig. 2, the obtained baryon asymmetry is  $Y_B = -\frac{28}{79} Y_{B-L} \sim 10^{-10}$ .

## 5. Conclusion

We have investigated the effect of  $A_4$  modular symmetry in explaining the neutrino oscillation phenomenology as well as baryon asymmetry of the universe through leptogenesis. The present model includes three right-handed and three left-handed heavy fermion fields to explore the neutrino phenomenology within the framework of linear seesaw. One of the important aspects of  $A_4$  modular symmetry is that the Yukawa couplings transform non-trivially, which leads to a specific flavor structure of the neutrino mass matrix. The flavor structure of heavy fermions gives rise to six doubly degenerate mass eigenstates and hence, to explain leptogenesis, we introduced a higher dimensional mass term for the right-handed fermions to generate a small mass splitting. We obtained a non-zero CP asymmetry from the decay of lightest heavy fermion eigen state. Using a specific benchmark of model parameters consistent with oscillation data, we solved coupled Boltzmann equations to obtain the evolution of lepton asymmetry, which comes out to be of the order  $\sim 10^{-10}$ , and hence, is sufficient to explain the present baryon asymmetry of the Universe.

## Acknowledgments

RM would like to acknowledge University of Hyderabad IoE project grant no. RC1-20-012.

## References

- [1] G. Altarelli, F. Feruglio, Nucl. Phys. B **741**, 215 (2006).
- [2] M.Hirsch, S.Morisi, J.W.F.Valle, Phys. Lett. B **679**, 454 (2009).
- [3] F. Feruglio, *Are neutrino masses modular forms?* arXiv:1706.08749.
- [4] T. Kobayashi, T. Nomura, T. Shimomura, Type II seesaw models with modular  $A_4$  symmetry, Phys. Rev. D **102**, 035019 (2020).
- [5] S.J.D. King, S. F. King, JHEP **09**, 043 (2020).
- [6] M. K. Behera, S. Mishra, S. Singirala, R. Mohanta, Phys. Dark Univ. **36**, 101027 (2022).
- [7] I. Esteban, M. C. Gonzalez-Garcia, A. Hernandez-Cabezudo, M. Maltoni, T. Schwetz, JHEP **01**, 106 (2019).
- [8] Planck Collaboration, N. Aghanim, et al., Astron. Astrophys. **641**, A6 (2020).
- [9] A. Pilaftsis, T. E. J. Underwood, Phys. Rev. D **72**, 113001 (2005).
- [10] T. Asaka, T. Yoshida, JHEP **09**, 089 (2019).
- [11] A. D. Sakharov, Sov. Phys. Usp. **34**, 392 (1991).
- [12] W. Buchmuller, P. Di Bari, M. Plumacher, Ann. Phys. **315**, 305 (2005).
- [13] M. Plumacher, Z. Phys. C **74**, 549 (1997).



- [14] G. F. Giudice, A. Notari, M. Raidal, A. Riotto, A. Strumia, Nucl. Phys. B **685**, 89 (2004).
- [15] S. Davidson, E. Nardi, Y. Nir, Phys. Rep. **466**, 105 (2008).
- [16] J. A. Harvey, M. S. Turner, Phys. Rev. D **42**, 3344 (1990).